

# Thermoelectrics

This work is licensed under a [Creative Commons Attribution-ShareAlike 4.0 International License](https://creativecommons.org/licenses/by-sa/4.0/).

**Kari Iltanen**

18.10.2011

kari.iltanen@smail.fi

Modified on 12.12.2019 for publication by removing images without redistribution rights.

Some of text published in Wikipedia earlier.

# Thermoelectricity

## Contents

1. Introduction	3
2. Transport theory	4
2.1 Electric conductivity	6
2.1.1 Scattering	8
2.1.2 Mobility	10
2.2 Thermal conductivity	11
2.2.1 Lattice thermal conductivity	11
2.2.2 Electronic thermal conductivity	15
2.3 Seebeck coefficient	16
2.4 Transport at nanoscale	17
3. Materials	20
3.1 Fabrication methods	21
3.2 Properties of thermoelectric materials	23
4. Characterization	27
4.1 Electrical measurements	27
4.2 Thermal measurements	28
4.3 Bands and crystal structure	30
4.4 Thermoelectric properties	31
5. Thermoelectric phenomenon in micro and nanoscale	31
5.1 Fabrication of thermoelectric nanomaterials	32
5.2 Material classes currently under investigation	33
5.3 Usage of nanoscale thermoelectrics	36
References	36

## 1. Introduction

Thermoelectric effect is based on the direct conversion of the temperature difference to voltage or vice versa. The conversion from the temperature difference to voltage is called a Seebeck effect. Peltier effect can be viewed as inverted Seebeck effect, which establishes a temperature difference with the electric current. Figure 1 shows a thermocouple that operates as a cooler or generator depending on whether the circuit has a power source or load. Both the Peltier and Seebeck effects require the use of two different materials. In Thomson effect, a wire with the temperature gradient between the ends becomes either heated or cooled depending on the material when the electric current goes through it. Although the Thomson effect itself has no practical applications, it has to be taken into account in detailed studies of other thermoelectric phenomena. Seebeck effect was observed for the first time in 1821, Peltier in 1834 and Thomson in 1851.

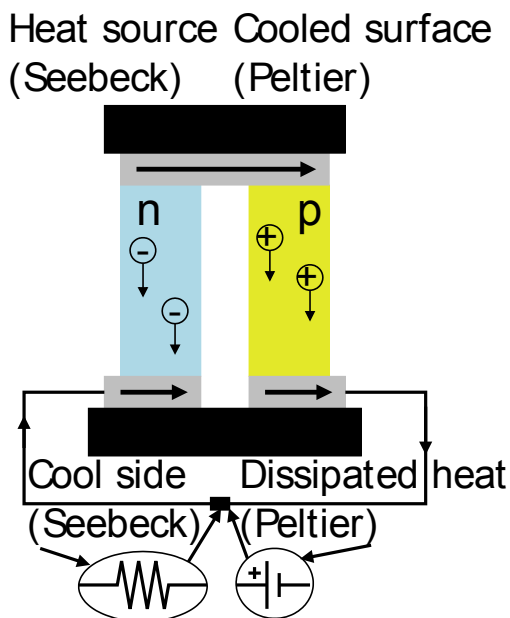


Figure 1. Semiconductor thermocouple that can be used as generator (Seebeck effect) or cooler (Peltier effect). Generator becomes cooler by switching the load (resistor) to power source. Arrows show the direction of electric current.

Seebeck coefficient is  $S(\alpha) = U/\Delta T$ , where  $U$  is the voltage generated by the temperature difference  $\Delta T$ . In metals, the value of the Seebeck coefficient is typically a few microvolts per Kelvin, in semiconductors the values from below  $100 \mu\text{V/K}$  even up to  $\sim 1 \text{ mV/K}$  are possible. The Peltier coefficient  $\Pi = I/q$ , where  $I$  is the electric current in a circuit and  $q$  is a rate of heating occurring at one junction, and  $-q$  is a rate of cooling at the other. The Thomson coefficient  $\beta = q/I\Delta T$ , where  $q$  is the rate of heat generated by the passage of current along the conductor with temperature difference  $\Delta T$ . These definitions are only valid when the temperature difference is small enough.

All three thermoelectric effects are linked by the Thomson (Kelvin) relationships, which were discovered by Lord Kelvin (Thomson) in 1854. The first Thomson relation  $S = \Pi/T$  links

Seebeck and Peltier coefficients. The second relation  $\frac{dS}{dT} = \frac{\beta_1 - \beta_2}{T}$  links Thomson coefficient to Seebeck coefficient, where subscripts indicate the two different materials used.

All thermoelectric coefficients discussed above depend on the magnetic field  $B$ . The Seebeck and Peltier coefficients have corresponding thermomagnetic coefficients, governed by the Nernst  $N$  and Ettinghausen  $P$  effects, respectively. In Nernst effect a transverse electric field  $E_y$  is produced by a longitudinal temperature gradient  $dT/dx$  in the presence of a magnetic field  $B_z$ . In Ettinghausen effect a longitudinal electric current  $I_x$  is produced by a transverse temperature gradient  $dT/dy$ . [1 (ch1)]

Thermoelectric phenomenon is in principle reversible thermodynamic process, but in practice non-idealities such as Joule heating will make the process irreversible. In the development of thermoelectric materials, normally the goal is to maximize the figure of merit ( $zT$ ), which depends on the electric and thermal conductivity and thermoelectric coefficient. Research on the thermoelectric phenomena began in the large scale the 1950s, but interest lasted only a few years and was reawakened after the nearly forty-year low activity period in the early 1990s.

The optimal thermoelectric material has been described by the term ‘phonon-glass-electron-crystal’, referring to the fact that lattice has low thermal conductivity like glass, but the electric properties are at the same level with crystal. In ordinary materials, all transport coefficients such as electric and thermal conductivities and Seebeck coefficient are coupled to each other, but in nanoscale this coupling is lost, allowing material parameters to be adjusted individually. Lattice thermal conductivity can be reduced significantly using nanoscale structures or complex crystal structure, since both increase phonon scattering and could cause phonon confinement, which can happen only at low temperatures in the nanometer scale structures.

## 2. Transport theory

Boltzmann equation

$$\frac{\partial f}{\partial t} + \mathbf{v} \cdot \nabla_r f - \frac{e}{\hbar} \boldsymbol{\delta} \cdot \nabla_k f = \left( \frac{\partial f}{\partial t} \right)_s$$

is normally the starting point in the analysis of transport problems in solids. The terms on the left hand-side are known as the drift terms of which the sum equals the scattering term on the right hand-side. In previous equation,  $f$  is a carrier distribution function and  $\boldsymbol{\delta}$  the electric field. If the solid in question is in thermal equilibrium and no external fields are present,  $f$  is the Fermi distribution. The scattering term in the equation in its most general form is complex as seen from the equation

$$\left( \frac{\partial f(\mathbf{k})}{\partial t} \right) = \frac{V}{(2\pi)^3} \int d\mathbf{k}' \left\{ [1 - f(\mathbf{k})] w_{\mathbf{k}\mathbf{k}'} f(\mathbf{k}') - [1 - f(\mathbf{k}')] w_{\mathbf{k}'\mathbf{k}} f(\mathbf{k}) \right\}.$$

The first term includes all scattering events from the occupied states  $\mathbf{k}$  to unoccupied states  $\mathbf{k}'$  and all scattering from  $\mathbf{k}'$  to state  $\mathbf{k}$  is included in the second term. The probability of electron to be scattered from a Bloch state  $\psi_{\mathbf{k}}(\mathbf{r})$  to a state  $\psi_{\mathbf{k}'}(\mathbf{r})$  is  $w_{\mathbf{k}\mathbf{k}'}$ .

This equation is usually solved by using the so-called relaxation time approximation, which assumes that the rate at which  $f$  returns to equilibrium distribution  $f_0$  is proportional to the deviation from  $f$  as stated in following equation

$$\left(\frac{\partial f}{\partial t}\right)_s = \frac{-f(k) - f_0(k)}{\tau(k)},$$

where  $\tau$  is the relaxation time.

In relaxation time approximation, it is assumed that the only role of scattering is in driving a non-equilibrium distribution back to thermal equilibrium. For a relaxation time method to work one has to be able to identify the relaxation rate from the scattering integrals the two distribution functions in it have to be separable, which is possible if the distribution functions came from same energy shell and thus it can be assumed that  $w_{kk'} = w_{k'k}$ . In elastic scattering previously mentioned conditions are true and the relaxation time method works, but for inelastic scattering  $w_{kk'} \neq w_{k'k}$ , which means that separation is not possible and therefore different methods have to be used. As  $\nabla_r f[k, T(r)] = (\partial f / \partial T) \nabla_r T$ , which comes from the chain rule for the gradient and when assuming only a small perturbation, one finds after linearization that

$$f(k) \approx f_0(k) + \frac{e}{\hbar} \delta \cdot \nabla_k f - \tau \frac{\partial f_0}{\partial T} v \cdot \nabla_r T.$$

The previous equation shows that thermal gradient can change  $f$  and is therefore associated with electric current thus describing together with thermodynamics thermoelectric effects. Normally, it is also assumed that even under non-equilibrium conditions the local equilibrium exist at much larger scales than that of the atomic dimensions. Because the equilibrium distribution function decreases and the distribution widens up as temperature increases, by using local equilibrium approximation it can be deduced that when thermal gradient increases, the non-equilibrium distribution decreases. [2, 3]

The transport properties of materials, which determine conductivities and thermoelectric coefficients, are usually described with the solutions of the Boltzmann transport equation, which is not valid in the nanometer scale when the wave effects come to play as it assumes that electron/phonon mean free path is much longer than its wavelength. This causes a need for a quantum transport model, which can couple scattering and quantum effects, as thermoelectric systems may often contain nanostructures. Even in bulk materials, there are uncertain-ties in various key transport parameters such as a phonon mean free path.

To understand the transport properties of nanomaterials, non-equilibrium Green's function (NEGF) formalism has to be used to explicitly take into account the quantum effects, though only a few such calculations have been done to this day. In NEGF, the idea is to seek a direct solution instead of statistical one to Schrödinger equation. NEGF describes the state and time evolution of the system. In the time domain, they are defined as the impulse response of the Schrödinger equation with the impulse being in this case an electron with particular energy. In the energy domain, we get the energy eigenvalues for the occupied eigenstates as a re-

sponse to the impulse. In addition, the available local electron density of states can be acquired from Green's functions. [4]

Modeling of transport behaviors in nanoscale materials is not yet possible, because models are still under development and require information about grain boundaries. While with transmission electron microscopy (TEM) individual atoms can be seen in solids, grain boundaries usually cannot currently be recognized from micrographs unless there is a big difference between atomic weights of different sides of the boundary. With the newest high resolution TEMs information about grain boundaries can be acquired but these studies have just started.

The models that are based on the Boltzmann equation with relaxation time approximation are currently used even to nanomaterials but they do not work properly when the quantum effects become significant and start giving even false predictions, such as decreasing thermal conductivity of extremely thin films as they come thinner. To use the Boltzmann equation even for nanostructures, the electron density of states and phonon dispersion relation should be determined first and then inserted to the equation. Lack of empirical information about nanoscale transport makes the development of necessary models difficult. [5]

Molecular dynamics (MD) simulators could be a potential tool for the investigation of transport processes in nanomaterials, but computational restrictions limit their usefulness by limiting the size of systems that can be investigated. Especially MD simulators that include quantum effects could be useful in the development of models to describe transport behavior at nanoscale that are even more computationally intensive than MD simulators based on classical physics with semi-classical potentials describing the strength of interatomic interactions. [5]

Simulations using Monte Carlo (MC) methods, usually the ensemble Monte Carlo (EMC) techniques can also be used to investigate transport processes in the materials. For short times, EMC approach provides more exact solutions to transport problems than Boltzmann equation, whose solution is achieved in the long time limit. Because the MC techniques use a random walk to simulate the stochastic motion of particles subject to collision processes, complicated physics can be introduced without additional complex formulations though usually the cost is increased need for computer time, which decreases the size of the systems that can be simulated. Advantages of the ensemble technique compared with normal MC procedures are the easier determination of the non-stationary time dependent evolution of the carrier distribution and appropriate ensemble averages. [3]

## 2.1 Electric conductivity

Electronic bandstructure determines electronic transport properties, such as electrical conductivity and thermoelectric coefficients, but has significance also for thermal properties. These bands form when an extremely large number ( $>10^{20}$ ) of atoms are brought together forming a solid, the number of molecular orbitals becomes large and energy difference between them becomes very small. Because the energy difference is comparable to energy exchanged with phonons and energy uncertainty from the Heisenberg uncertainty principle  $\Delta E \Delta t \gtrsim h$  for quite long time intervals, separation of the energy levels within the band does not matter. The uncertainty principle states that energy level is in fact an narrow energy interval centering

around said level, with the width of the interval depending on time it exist unperturbed. Figure 2 shows how the bands form from the discrete energy levels of single atoms.

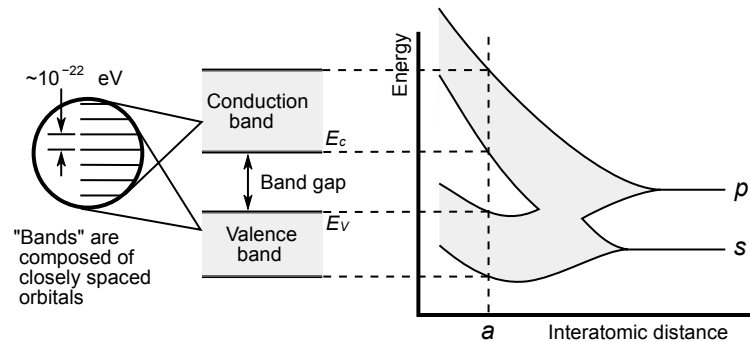


Figure 2. Discrete energy levels broaden as large number of identical atoms approach each other,  $a$  is equilibrium separation of chemically bound atoms. Source:

<https://commons.wikimedia.org/w/index.php?>

title=File:Solid\_state\_electronic\_band\_structure.svg&oldid=367284686

Degenerate (highly doped) semiconductors behave more like metals than normal semiconductors due to high carrier concentration. Bandgap also becomes narrower because the function describing density of states is perturbed due to strong charge induced local fields. This results bandtail states, which can be thought as 'tail' for normal band meaning extra states beyond band minima or maxima. In degenerate semiconductors, the Fermi-level is within the conduction or valence band meaning that the ionization energy of the impurity centers drops to zero. Impurities also form bands when their concentration rises to level  $10^{19}$   $\text{cm}^{-3}$ . Band-structure of highly doped semiconductor is shown in Figure 3. [6]

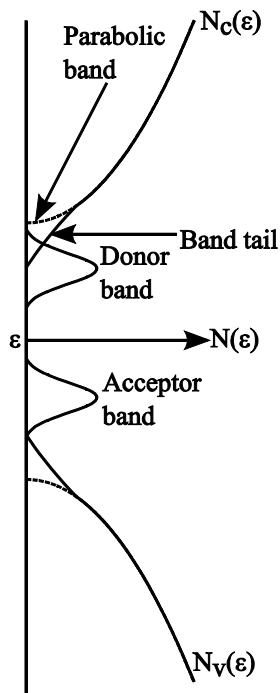


Figure 3. Schematic illustration of effects of heavy doping to bandstructure. Bandgap narrowing is caused by bandtails and bands formed by doping atoms are also illustrated in figure.

The effective mass of charge carriers, concentration and thermoelectric coefficients are all determined by the bandstructure. The carrier mobility is determined mainly by collisions and lattice scattering events. Effective masses depend on the shape of the bands as stated in the

following equation  $m_e^* = \hbar^2 \left( \frac{d^2 \epsilon}{d^2 k} \right)^{-1}$ , where  $k$  is a wave vector and  $\epsilon$  is energy. Density of

states effective mass ( $m_d^*$ ), which is the mass used in the density of states calculations, is a geometric mean of principal effective masses ( $m_x^*, m_y^*, m_z^*$ ), but in lower dimensional systems the effective mass in the direction of confinement is not included. For a 3D case with a single band, it is expressed with the following equation  $m_d^* = \sqrt[3]{m_x^* m_y^* m_z^*}$ . [7]

Carrier concentration is one of the most important factors for electrical conductivity. If temperature is high enough so that most dopant atoms are ionized and doping level is much higher than the intrinsic carrier concentration, then as a good approximation the total carrier concentration is equal to the doping level value. [6]

Only a partially filled band enables conduction. The main excitation mechanism is thermal so that semiconductors show strong thermal dependence in the electrical conductivity. Fermi-Dirac distribution  $f(\epsilon)$  governs the occupation probability of electronic states in equilibrium in semiconductors. The function for the density of states  $N(\epsilon)d(\epsilon)$  tells the number of available quantum states in the energy interval between  $\epsilon$  and  $\epsilon+d(\epsilon)$ . Intrinsic carrier density for electrons in conduction band can be calculated from the following integral

$$n_0 = \int_{\epsilon_c}^{\infty} N(\epsilon) f(\epsilon) d(\epsilon).$$

The Fermi-level  $E_F$  depends on  $T$  and carrier density. In extrinsic (doped) semiconductors,  $E_F$  depends mainly on  $T$  and decreases as temperature increases, because  $n$  remains almost constant as a function of temperature. In intrinsic (undoped) semiconductors,  $n$  varies significantly with  $T$  and  $E_F$  remains almost constant in the middle of bandgap. Dependencies on  $E_F$  can also change with the density of states. [1, 7]

Flow of the electric current is caused by external fields as a driving force for charge carriers. Electrical resistance is caused by scattering of charge carriers from many different targets such as other carriers, phonons, defects and impurities. Scattering is divided into elastic and inelastic scattering. [2, 6]

### 2.1.1 Scattering

Elastic scattering means that energy is (almost) conserved during the scattering event. Some elastic scattering processes are scattering from acoustic phonons, impurity scattering, piezoelectric scattering, etc. In acoustic phonon scattering, electrons scatter from state  $\mathbf{k}$  to  $\mathbf{k}'$ , while emitting or absorbing a phonon of wave vector  $\mathbf{q}$ . This phenomenon is usually modeled by assuming that lattice vibrations cause small shifts in energy bands. The additional potential causing the scattering process is generated by the deviations of bands due to these small transitions from frozen lattice positions. [3]

Piezoelectric effect can occur only in compound semiconductor due to their polar nature. It is small in most semiconductors but may lead to local electric fields that cause scattering of car-



riers by deflecting them, this effect is important mainly at low temperatures where other scattering mechanisms are weak. These electric fields arise from the distortion of the basic unit cell as strain is applied in certain directions in the lattice.

Ionized impurities create local Coulomb potential changes that lead to scattering of electrons. When determining the strength of these interactions due to the long-range nature of the Coulomb potential, other impurities and free carriers cause the range of interaction with the carriers to reduce significantly compared to bare Coulomb interaction. [3]

If these scatterers are near the interface, the complexity of the problem increases due to the existence of crystal defects and disorders. Charge trapping centers that scatter free carriers form in many cases due to defects associated with dangling bonds. Scattering happens because after trapping a charge, the defect becomes charged and therefore starts interacting with free carriers. If scattered carriers are in the inversion layer at the interface, the reduced dimensionality of the carriers makes the case differ from the case of bulk impurity scattering as carriers move only in two dimensions. Interfacial roughness also causes short-range scattering limiting the mobility of quasi two-dimensional electrons at the interface.

Surface roughness scattering caused by interfacial disorder is short range scattering limiting the mobility of quasi two-dimensional electrons at the interface. From high-resolution transmission electron micrographs, it has been determined that the interface is not abrupt on the atomic level, but actual position of the interfacial plane varies one or two atomic layers along the surface. These variations are random and cause fluctuations of the energy levels at the interface, which then causes scattering. [3]

In compound (alloy) semiconductors, which many thermoelectric materials are, scattering caused by the perturbation of crystal potential due to the random positioning of substituting atom species in a relevant sublattice is known as alloy scattering. This can only happen in ternary or higher alloys as their crystal structure forms by randomly replacing some atoms in one of the cubic lattices (sublattice) that form zinc-blende structure. Generally, this phenomenon is quite weak but in certain materials or circumstances, it can become dominant effect limiting conductivity. In bulk materials, interface scattering is usually ignored. [2, 3, 4, 6]

During inelastic scattering processes, significant energy exchange happens. As with elastic phonon scattering also in the inelastic case, the potential arises from energy band deformations caused by atomic vibrations. Optical phonons causing inelastic scattering usually have the energy in the range 30-50 meV, for comparison energies of acoustic phonon are typically less than 1 meV but some might have energy in order of 10 meV. There is significant change in carrier energy during the scattering process. Optical or high-energy acoustic phonons can also cause intervalley or interband scattering, which means that scattering is not limited within single valley. [3]

Due to the Pauli exclusion principle, electrons can be considered as non-interacting if their density does not exceed the value  $10^{17} \text{ cm}^{-3}$  or electric field value  $10^3 \text{ V/cm}$ . However, significantly above these limits electron-electron scattering starts to dominate. Long range and nonlinearity of the Coulomb potential governing interactions between electrons make these interactions difficult to deal with. [2, 3, 4]

### 2.1.2 Mobility

The mobility  $\mu$  is defined as the magnitude of the mean drift velocity  $v_D$  per unit field  $E$  and therefore has the form  $\mu = \frac{v_D}{E} = \frac{-q\tau_C}{m^*}$ , where  $m^*$  is the effective mass and  $\tau_C$  relaxation time and  $-q$  is the charge of electron if the electric field is not too strong (Ohm's law valid). Electrical conductivity ( $\sigma$ ) is proportional to the product of the mobility and carrier concentration, the formula is  $\sigma = ne\mu$  ( $e$  is elementary charge and  $n$  carrier concentration) for materials that have only electron conduction. If holes are the charge carriers,  $n$  is replaced with the hole concentration  $p$  and hole mobility is used instead of electron mobility. In semiconductors, both the electron and hole conductivities are summed together to get the total conductivity. In strong electric fields (typically above  $10^4$ - $10^5$  V/cm), the drift velocity saturates and the mobility drops.

The total mobility is the function of temperature and is given by the Matthiesen's rule, where  $\frac{1}{\mu} = \frac{1}{\mu_I} + \frac{1}{\mu_p}$   $\mu_I$  is the mobility limited by impurity scattering and  $\mu_p$  is the mobility limited by phonon scattering. This rule is not valid if the factors affecting the mobility depend on with each other, because individual scattering probabilities cannot be summed unless they are independent of each other. The average free time of flight of a carrier and therefore the relaxation time is inversely proportional to the scattering probability. [2, 3, 6]

As  $\frac{1}{\tau} \propto \langle v \rangle \Sigma$ , where  $\Sigma$  is the scattering cross section for electrons and holes at a scattering center and  $\langle v \rangle$  is a thermal average (Boltzmann statistics) over all electron or hole velocities in the lower conduction band or upper valence band, temperature dependence of the mobility can be determined. In here, the following definition for the scattering cross section is used: number of particles scattered into solid angle  $d\Omega$  per unit time divided by number of particles per area per time (incident intensity), which comes from classical mechanics. As Boltzmann statistics are valid for semiconductors  $\langle v \rangle \sim \sqrt{T}$ .

For scattering from acoustic phonons for temperatures  $T \gg \Theta$  ( $\Theta$ =Debye temperature), the estimated cross section  $\Sigma_{ph}$  is determined from the square of the average vibrational amplitude of a phonon to be proportional to  $T$ . The scattering from charged defects (ionized donors or acceptors) leads to the cross section  $\Sigma_{def} \propto \langle v \rangle^{-4}$ . This formula is the scattering cross section for "Rutherford scattering", where a point charge (carrier) moves past another point charge (defect) experiencing Coulomb interaction.

The temperature dependencies of these two scattering mechanism in semiconductors can be determined by combining formulas for  $\tau$ ,  $\Sigma$  and  $m_{de}^*$ , to be for scattering from acoustic phonons  $\mu_{ph} \propto T^{-3/2}$  and from charged defects  $\mu_c \propto T^{3/2}$ . The mobility as a function of temperature in a generic semiconductor is shown in Figure 4. [2, 6]

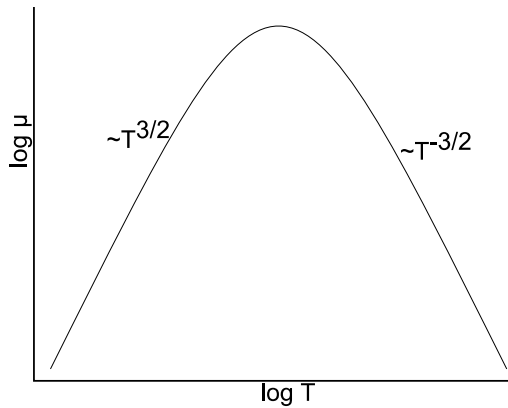


Figure 4. Schematic temperature dependence of mobility in semiconductors due ionized defects and pho-nons.

## 2.2 Thermal conductivity

Free electrons and phonons are responsible for the heat transport in solids, but what is the one that dominates depends on the type of material. In metals, electronic contribution dominates, but on the other hand in insulators and semiconductors, the phonon heat conduction dominates. Thermal conductivity is a nonequilibrium phenomenon. A thermal current can only arise if a temperature gradient is present. The thermal current density  $Q$  is proportional to the temperature gradient  $Q = -\lambda \text{grad } T$ , where  $\lambda$  is thermal conductivity. [2]

### 2.2.1 Lattice thermal conductivity

By assuming harmonic oscillation of lattice atoms, differential equations for the positions of all atoms can be written. If the lattice has  $n$  unit cells each with  $r$  atoms, one has  $3rN$  differential equations to solve. With plane wave approximation and using translational symmetries, this complex system simplifies to the linear homogeneous system of the order of  $3r$ . This system has solutions only if its determinant vanishes. The resulting equation has  $3r$  solutions,  $\omega(q)$ , for each  $q$ . The dispersion relation describes dependence of  $\omega$  from the wave vector  $q$ . The so called branches of the dispersion relation are the  $3r$  different solutions. Branches that go to zero at small  $q$  are called acoustical branches and those for which  $\omega(q) \neq 0$  at  $q=0$  are called optical branches (Figure 5). [2]

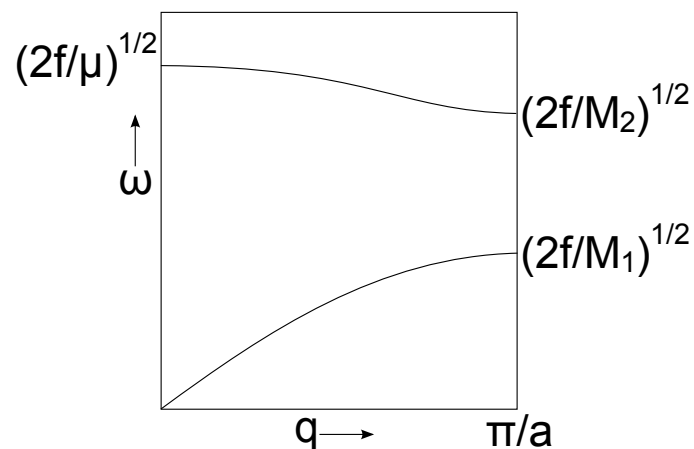


Figure 5. Phonon dispersion curve for diatomic chain,  $2f$  is force constant,  $1/\mu = 1/M_1 + 1/M_2$ ,  $a$  is the distance between atoms of same type.

Phonons in the acoustical branch dominate the phonon heat conduction as they have greater energy dispersion and therefore a greater distribution of phonon velocities. Additional optical modes could also be caused by the presence of internal structure (i.e., charge or mass) at a lattice point; it is implied that the group velocity of these modes is low and therefore their contribution to the lattice thermal conductivity  $\lambda_L$  ( $\kappa_L$ ) is small. [7]

Each phonon mode can be split into one longitudinal and two transverse polarization branches. By extrapolating the phenomenology of lattice points to the unit cells it is seen that the total number of degrees of freedom is  $3pq$  when  $p$  is the number of primitive cells with  $q$  atoms/unit cell. From these only  $3p$  are associated with the acoustic modes, the remaining  $3p(q-1)$  are accommodated through the optical branches. This implies that structures with larger  $p$  and  $q$  contain a greater number of optical modes and a reduced  $\lambda_L$ .

From these ideas, it can be concluded that increasing crystal complexity, which is described by a complexity factor  $CF$  (defined as the number of atoms/primitive unit cell), decreases  $\lambda_L$ . Micheline Roufosse and P.G. Klements derived the exact proportionality in their article Thermal Conductivity of Complex Dielectric Crystals at Phys. Rev. B 7, 5379–5386 (1973). This was done by assuming that the relaxation time  $\tau$  decreases with increasing number of atoms in the unit cell and then scaling the parameters of the expression for thermal conductivity in high temperatures accordingly. [7]

Specific heat capacity  $c_v$  is a temperature derivative of the internal energy  $U(T)$ , which is the total energy of solid in thermal equilibrium. Density of states  $Z$  and the thermal energy  $\varepsilon(\omega, T)$  of an oscillator with frequency  $\omega$ , allow writing the following expression

$$U(T) = \frac{1}{V} \int_0^{\infty} Z(T) \varepsilon(\omega, T) d\omega.$$

Debye approximation imposes common cutoff frequency, which is determined by the requirement that the total number of states is equal to  $3rN$ , for all three acoustic modes. Therefore,

$$c_v(T) = \frac{9rN}{V} \frac{1}{\omega_D^3} \frac{d}{dT} \int_0^{\omega_D} \frac{\hbar \omega^3 d\omega}{e^{\hbar\omega/kT} - 1}$$

from where by changing upper integration limit to infinity and marking  $\hbar \omega_D = k \Theta$  one arrives to final form for  $c_v$ . This approximation is valid only at very low temperatures when only elastic waves are excited and give the specific heat the  $T^3$  dependence as stated in the following equation

$$c_v(T) = \frac{1}{V} 3rNk \frac{4\pi^4}{5} \left( \frac{T}{\Theta} \right)^3,$$

which is valid when  $T \ll \Theta$ , where  $\Theta$  is the Debye temperature,  $3rN$  is total number of states,  $k$  is the Boltzmann constant and  $V$  is volume. [2]

Describing of anharmonic effects is complicated because exact treatment as in the harmonic case is not possible and phonons are no longer exact eigensolutions to the equations of motion. Even if the state of motion of the crystal could be described with a plane wave at a particular time, its accuracy would deteriorate progressively with time. Time development would

have to be described by introducing a spectrum of other phonons, which is known as the phonon decay. The two most important anharmonic effects are the thermal expansion and the phonon thermal conductivity.

Only when the phonon number  $\langle n \rangle$  deviates from the equilibrium value  $\langle n \rangle^0$ , can a thermal current arise as stated in following expression

$$Q_x = \frac{1}{V} \sum_{q,j} \hbar \omega (\langle n \rangle - \langle n \rangle^0) v_x,$$

where  $v$  is the energy transport velocity of phonons. Only two mechanisms exist that can cause time variation of  $\langle n \rangle$  in a particular region. The number of phonons that diffuse into the region from neighboring regions differs from those that diffuse out, or phonons decay inside the same region into other phonons. A special form of the Boltzmann equation

$$\frac{d\langle n \rangle}{dt} = \left. \frac{\partial \langle n \rangle}{\partial t} \right|_{diff.} + \left. \frac{\partial \langle n \rangle}{\partial t} \right|_{decay}$$

states this. When steady state conditions are assumed the total time derivate of phonon number is zero, because the temperature is constant in time and therefore the phonon number stays also constant. Time variation due to phonon decay is described with a relaxation time ( $\tau$ ) approximation

$$\left. \frac{\partial \langle n \rangle}{\partial t} \right|_{decay} = \frac{-\langle n \rangle + \langle n \rangle^0}{\tau},$$

which states that the more the phonon number deviates from its equilibrium value, the more its time variation increases. At steady state conditions and local thermal equilibrium are assumed we get the following equation

$$\left. \frac{\partial \langle n \rangle}{\partial t} \right|_{diff.} = -v_x \frac{\partial \langle n \rangle^0}{\partial T} \frac{\partial T}{\partial x}.$$

Using the relaxation time approximation for the Boltzmann equation and assuming steady-state conditions, the phonon thermal conductivity  $\lambda_L$  can be determined. The temperature dependence for  $\lambda_L$  originates from the variety of processes, whose significance for  $\lambda_L$  depends on the temperature range of interest. Mean free path is one factor that determines the temperature dependence for  $\lambda_L$ , as stated in the following equation

$$\lambda_L = \frac{1}{3V} \sum_{q,j} v(q,j) \Lambda(q,j) \frac{\partial}{\partial T} \varepsilon[\omega(q,j), T],$$

where  $\Lambda$  is the mean free path for phonon. This equation is a result of combining the four previous equations with each other and knowing that  $\langle v_x^2 \rangle = \frac{1}{3} v^2$  for cubic or isotropic systems and  $\Lambda = v\tau$ . [2]

At low temperatures ( $<10$  K) the anharmonic interaction does not influence the mean free path and therefore, the thermal resistivity is determined only from processes for which q-conservation does not hold. These processes include the scattering of phonons by crystal defects, or the scattering from the surface of the crystal in case of high quality single crystal.

Therefore, thermal conductance depends on the external dimensions of the crystal and the quality of the surface. Thus, temperature dependence of  $\lambda_L$  is determined by the specific heat and is therefore proportional to  $T^3$ . [2]

Phonon quasimomentum is defined as  $\hbar q$  and differs from normal momentum due to the fact that it is only defined within an arbitrary reciprocal lattice vector. At higher temperatures ( $10\text{ K} < T < \Theta$ ), the conservation of energy  $\hbar \omega_1 = \hbar \omega_2 + \hbar \omega_3$  and quasimomentum  $q_1 = q_2 + q_3 + G$ , where  $q_1$  is wave vector of the incident phonon and  $q_2, q_3$  are wave vectors of the resultant phonons, may also involve a reciprocal lattice vector  $G$  complicating the energy transport process. These processes can also reverse the direction of energy transport.

Therefore, these processes are also known as Umklapp (U) processes and can only occur when phonons with sufficiently large  $q$ -vectors are excited, because unless the sum of  $q_2$  and  $q_3$  points outside of the Brillouin zone the momentum is conserved and the process is normal scattering (N-process). The probability of a phonon to have energy  $E$  is given by the Boltzmann distribution  $P \propto e^{-E/kT}$ . To U-process to occur the decaying phonon to have a wave vector  $q_1$  that is roughly half of the diameter of the Brillouin zone, because otherwise quasimomentum would not be conserved.

Therefore, these phonons have to possess energy of  $k\Theta/2$ , which is a significant fraction of Debye energy that is needed to generate new phonons. The probability for this is proportional to  $e^{-\Theta/bT}$ , with  $b=2$ . Temperature dependence of the mean free path has an exponential form  $e^{\Theta/bT}$ . The presence of the reciprocal lattice wave vector implies a net phonon backscattering and a resistance to phonon and thermal transport resulting finite  $\lambda_L$  [7], as it means that momentum is not conserved. Only momentum non-conserving processes can cause thermal resistance. [2]

At high temperatures ( $T > \Theta$ ) the mean free path and therefore  $\lambda_L$  has a temperature dependence  $T^{-1}$ , to which one arrives from formula  $e^{\Theta/bT}$  by making the following approximation  $e^x \propto x, |x| < 1$  and writing  $x = \Theta/bT$ . This dependency is known as Eucken's law and originates from the temperature dependency of the probability for the U-process to occur. Figure 6 shows the characteristic behavior of thermal conductivity in quartz as a function of temperature. [2, 7]

(image removed due copyright, originally Figure 5.7 on [2])

Figure 6. Schematic representation of thermal conductivity of quartz as crystalline, after neutron bombardment and as amorphous. [2]

Thermal conductivity is usually described by the Boltzmann equation with the relaxation time approximation in which phonon scattering is a limiting factor. Another approach is to use analytic models or molecular dynamics or Monte Carlo based methods to describe thermal conductivity in solids.

Short wavelength phonons are strongly scattered by impurity atoms if an alloyed phase is present, but mid and long wavelength phonons are less affected. Mid and long wavelength phonons carry significant fraction of heat, so to further reduce lattice thermal conductivity one has to introduce structures to scatter these phonons. This is achieved by introducing interface

scattering mechanism, which requires structures whose characteristic length is longer than that of impurity atom. Some possible ways to realize these interfaces are nanocomposites and embedded nanoparticles/structures. More on possible structures will be on chapter 5.2. [5]

### 2.2.2 Electronic thermal conductivity

Hot electrons from higher energy states carry more thermal energy than cold electrons, while electrical conductivity is rather insensitive to the energy distribution of carriers because the amount of charge that electrons carry, does not depend on their energy. This is a physical reason for the greater sensitivity of electronic thermal conductivity to energy dependence of density of states and relaxation time, respectively. [7]

The Wiedemann-Franz law

$$\lambda_E = \frac{\pi^2}{3} \left( \frac{k}{e} \right)^2 \sigma T = L \sigma T,$$

where  $\sigma$  is electrical conductivity, describes the thermal conductivity of electrons in metals. This law connects electric conductivity to thermal conduction by charge carriers and temperature. Therefore, it complicates the decreasing of thermal conductivity once the lattice thermal conductivity has been reduced. In degenerate semiconductors, the Lorenz number  $L$  has a strong dependency on certain system parameters: dimensionality, strength of interatomic interactions and Fermi-level. This law is not valid or the value of the Lorenz number can be reduced at least in following cases: manipulating electronic density of states, varying doping density and layer thickness in superlattices and materials with correlated carriers. [5, 7]

Mahan and Sofo have showed in their article *The best thermoelectric* (*PNAS* 1996 93 (15) 7436-7439) that materials with a certain electron structure have reduced electron thermal conductivity. Based on their analysis one can demonstrate that if the electron density of states in the material is close to the delta-function, the electronic thermal conductivity drops to zero. By taking the following equation  $\lambda_E = \lambda_0 - T \sigma S^2$ , where  $\lambda_0$  is the electronic thermal conductivity when the electrochemical potential gradient inside the sample is zero, as a starting point.

As next step the transport coefficients are written as following  $\sigma = \sigma_0 I_0$ ,  $\sigma S = \left( \frac{k}{e} \right) \sigma_0 I_1$ ,

$\lambda_0 = \left( \frac{k}{e} \right)^2 \sigma_0 T I_2$ , where  $\sigma_0 = e^2 / (\hbar a_0)$ , with  $a_0$  as the Bohr's radius. The dimensionless inte-

grals  $I_n$  are defined as  $I_n = \int_{-\infty}^{\infty} \frac{e^x}{(e^x + 1)^2} s(x) x^n dx$ , where  $s(x)$  is the dimensionless transport

distribution function. The integrals  $I_n$  are the moments of the function

$P(x) = D(x) s(x)$ ,  $D(x) = \frac{e^x}{(e^x + 1)^2}$ ,  $x$  is the energy of carriers. By substituting the previous for-

mulas for the transport coefficient to the equation for  $\lambda_E$  we get the following equation

$\lambda_E = \left( \frac{k}{e} \right)^2 \sigma_0 T \left( I_2 - \frac{I_1^2}{I_0} \right)$ . From the previous equation we see that  $\lambda_E$  to be zero the bracketed

term containing  $I_n$  terms have to be zero. Now if we assume that  $s(x) = f(x) \delta(x - b)$ , where  $\delta$



is the Dirac delta function,  $I_n$  terms get the following expressions  $I_0 = D(b)f(b)$ ,  $I_1 = D(b)f(b)b$ ,  $I_2 = D(b)f(b)b^2$ . By substituting these expressions to the equation for  $\lambda_E$ , we see that it goes to zero. Therefore,  $P(x)$  has to be delta function. Table 1 lists lattice and electric thermal conductivities and their ratios in some materials. [5]

Table 1. Lattice and electric thermal conductivities and their ratios in some materials at room temperature (300 K). Values acquired from various publications, textbooks, and handbooks.

material	$\lambda_L$ (W/(m*K))	$\lambda_E$ (W/(m*K))	$\lambda_L / \lambda_E$
W	5.0	168	0.030
Cu	13	388	0.033
Si	113	36	3.1
Ge	63	0.6	105
BiTe	1.6	0.4	4
InAs	30	1.5	20
PbTe	2.0	0.3	6.7

### 2.3 Seebeck coefficient

Seebeck effect comprises from multiple distinct physical processes, but the most important of them is the diffusion of electrons. Only portions of the band close to  $E_F$  have significant impact on the thermoelectric properties of material. Under this approximation many materials such as Si can be classified as single band materials. In single band materials with parabolic bands Seebeck coefficient  $S$  is proportional to the difference between the electron average energy weighted by the relaxation time and  $E_F$ . In multi band materials such as intrinsic semiconductors and semimetals  $S$  from each band has to be taken into account separately. [7]

Electron-phonon interactions, which refer to the dependence of electronic energy levels on the position of atoms in a solid, have significant impact on Seebeck coefficient. Therefore, thermal expansion alters electronic states of a solid. Electronic energy levels are also temperature dependent due to the shift of atoms in solids from equilibrium positions and change in carrier energies caused by electron-lattice interactions altering lattice vibration amplitudes.

The phenomenon known as phonon-drag becomes a significant contributor for the Seebeck coefficient at low temperatures ( $\sim 50$  K), which is caused by interactions between carriers and sound waves, carriers impart momentum to sound waves that is not readily dissipated. Seebeck coefficient rises as temperature decreases due the diminishing of the scattering of sound waves by phonons. [1 (ch5)]

Phonon-drag contribution is then determined by the following equation  $\alpha_{transport} = \frac{k}{q} \left( \frac{s^2 \tau}{D} \right) f$ ,

where  $q$  is the charge of the carrier,  $s$  is the sound velocity,  $f$  is the fraction of momentum of a carrier that is transferred to the sound waves and  $\tau$  is the relaxation time for the dissipation of sound waves' momentum through their interactions with atoms. For the diffusion constant of carriers  $D$ , the Einstein definition is used  $\langle v \rangle \sim \sqrt{T}$ . Both  $\tau$  and  $\alpha_{transport}$  in previous equation increase with decreasing  $T$ . [1 (ch5)]



At certain point, carriers become predominant scatterers of sound waves and therefore phonon-drag contribution drops with decreasing temperature. In this region, the previous equation is not valid anymore and the following equation  $\alpha_{transport} = \frac{k}{q} \left[ \frac{N(T)}{n} \right]$  has to be used,

where  $N(T)$  is the density of acoustic phonons interacting strongly with charge carriers whose density is  $n$ .

The interaction between carriers and phonons is at strongest when they have comparable wavelengths. Therefore, the density of phonon states is essentially equal to the density of thermally accessible carrier states. These densities and  $\alpha_{transport}$  both decrease with temperature and eventually drop to zero. Therefore, phonon-drag produces a peak to the Seebeck coefficient as a function of temperature. [1 (ch5)]

Polaron is quasiparticle comprising of carrier and polarization region surrounding it. The polarization occurs when atoms move slightly from their equilibrium positions due to their interactions with the carrier. The atoms return to their original positions when the carrier has passed. If the carrier moves too fast, atoms do not have enough time to change their positions in response to the presence of the carrier. The so called polaron formation occurs frequently in materials with ionic bonds, because their electron-lattice interactions have a long range and exceptional strength rendering them especially effective. It can also happen in material with covalent bonds if imposed disorder slows carriers enough.

The polaron moves slower than the carrier, because its movement is controlled by changing potential associated with surrounding atoms. Polaron motion is described as a series of thermally assisted hops, if it is incoherent. This happens, when the strain energy related carrier moving between adjacent sites exceeds electronic transfer energy. Contribution of this phenomenon to Seebeck coefficient depends on the polaron energy and strength of electron-lattice coupling. [1 (ch5)]

## 2.4 Transport in nanoscale

Effects of quantum confinement start to dominate the electric properties of materials when the carrier mean free path (~20-40 nm) becomes comparable with the size of the structures. In nanoscale, phonon dispersion relations and frequency distribution start also to change due to the confinement. In superlattices the phonon band gaps may form due to zone folding, if the phonon mean free path spans multiple interfaces (>10). This is due to interference of the waves reflected from multiple interfaces. In quantum wells with the width  $d$  in  $z$ -direction with no phonon wavevector component in the  $y$ -direction, three different types of acoustic modes exist, which have different dispersion relations. The modes in question are referred as shear waves (S), dilatational waves (D), flexural waves (F). [1 (ch14), 8]

The dispersion relation for the shear waves is  $\omega_n = s_t (q_x^2 + q_{zn}^2)^{1/2}$ , where  $q_{zn} = \pi n / d$  and  $n$  is an index referring to different branches of the same polarization. For the other modes (D and F) the dispersion relation is the following  $\omega_n = v_l (q_x^2 + q_l^2)^{1/2}$ , where  $v_l$  is the speed of the longitudinal elastic waves in the bulk. However, these effects become significant only when the size of the structures is comparable to the phonon wavelength, which is usually from 1 to 2 nm for typical TE-materials at the temperatures of interest. Dominating scattering

mechanism may also change in nanoscale structures. Depending in how many dimensions the carrier movement takes place, the density of states takes different shapes. [1 (ch14)]

The energy dependence of the density of states is  $D \propto E^x$ , where x changes from +1/2 to 0 and -1/2 as system dimensions change from 3D to 2D and 1D. In 1D and 0D systems, the density of states is higher at certain energy values than in the bulk material, but bands are narrower. This behavior is demonstrated in figure 7. In 2D and 1D systems, the density of states is inversely proportional to quantum well/wire thickness a. [1 (ch16), 6, 7]

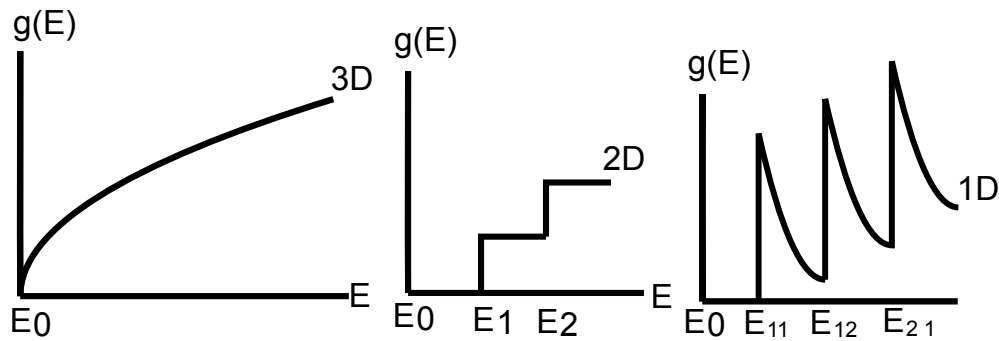


Figure 7. Density of states,  $g(E)$ , for 3D, 2D, and 1D electron gas in bulk material, quantum well, and quantum wire, respectively. The staggered pattern comes from the superposition of multiple sub-bands, the shifts upward from the bulk ground state ( $E_0$ ) correspond to the confinement energy ( $E_1, E_2$ , etc.).

Effective bandgap also increases due to the upward(/downward) shift of conduction(/valence) band ground states corresponding to the confinement potential energy which is inversely proportional to a and  $m_d$ . Average electron energy is smaller in confined systems than in bulk systems if both have the same Fermi-energy due to the shape of bands. If carrier concentration and temperature stay the same, material with a larger density of states will have a smaller Fermi-energy.

The Seebeck coefficient decreases as  $E_F$  increases or T decreases. Starting from basic definitions for the transport coefficients P. Pichanusakorn and P. Banduru have determined the following equation for the diffusive Seebeck coefficient

$$S = \pm \frac{k}{e} \left( \frac{(r + (D/2) + 1) F_{r + \frac{D}{2}}(\eta)}{(r + (D/2)) F_{r + \frac{D}{2} - 1}(\eta)} - \eta \right),$$

where r is characteristic “scattering constant” and usually experimentally determined, D is the “dimensionality” factor,  $F_j$  is the jth order Fermi integral and  $\eta = \frac{(E_F - E_0)}{kT}$ , where  $E_0$  is the energy of the bottom of the conduction band [7].

In extrinsic semiconductors increasing temperature causes  $E_F$  to move toward the middle of the band gap, where it is in intrinsic semiconductors, therefore raising the magnitude of Seebeck coefficient. As temperature rises more and more electrons move to the conduction band thus decreasing relative impact of doping to transport properties and therefore the semiconductor becomes more intrinsic. [5, 7]

For a nondegenerate semiconductor, the following formulas can be used describe the dependencies of  $E_F$ : for n-type  $E_F = E_C - kT \ln \frac{N_C}{N_D}$  and for p-type  $E_F = E_V + kT \ln \frac{N_V}{N_A}$ , where  $N_C$  and  $N_V$  are the effective density of states in the conduction and valence bands respectively,  $N_D$  and  $N_A$  are concentrations of dopant atoms.  $N_C$  and  $N_V$  came from the following expression  $N_C = 2 \left( \frac{2 \pi m_{de}^* kT}{h^2} \right)^{3/2}$ , where  $m_{de}^*$  is the density of states effective mass for the conduction band, to get  $N_V m_{de}^*$  has to be replaced with the corresponding parameter for the valence band. It is also assumed that all dopants are ionized. These formulas are determined by calculating carrier concentration in the band from density of states and occupation probability. If the Fermi-level is in deep within the band gap so that condition  $|E_{C(V)} - E_F| \geq 3kT$  is satisfied, the Fermi distribution can be approximated with the Boltzmann distribution.

Seebeck coefficient can also be increased by energy filtering, where an additional scattering mechanism is introduced to preferentially scatter low energy electrons, which have negative contribution to the Seebeck coefficient, to minimize their contribution to transport properties. In nanocomposites, this can be achieved though electron grain boundary scattering. Though this effect decreases electrical conductivity, power factor  $S^2 \sigma$  can be increased if increase of Seebeck coefficient compensates for the decreased electrical conductivity. [5, 7]

A ballistic transport phenomenon appears in nanoscale and means that electron or phonon can travel through entire wire without scattering at all. This is known to occur in nanotubes and wires if the length of the channel is much smaller than electron mean free path and the diameter is order of the electron wavelength and enables very high conductivities. However, the wire has finite non-zero resistance, which is referred as contact resistance. The resistance originates from the interface between the conductor and the contacts, which are different materials. Inside the conductor only a few current carrying modes (subbands) exist so the current has to be redistributed from infinitely many modes from contacts at the interface leading to interface resistance. [2, 9]

Because electrons maintain their Bloch-wave nature in z-direction one-dimensional bands (subbands) exist for the each allowed pair  $k_x, k_y$ . Each of these subbands carries the same current that is determined by the universal conductance  $G_0 = \frac{2e^2}{h} = 7.74809 \times 10^{-5} \Omega^{-1}$  and by the voltage between the contacts. It should be noted that the value of  $G_0$  drops to half if spin-degeneracy is lost, because the number of available states drops to half. The number of conduction channels and subband current determines the ballistic current in wire. [2]

In multi quantum well structures and in some superlattices the tunneling may have a significant impact on the device performance. Tunneling between quantum wells causes discrete energy levels to form minibands. This phenomenon is comparable to formation of bands in the bulk material. If one wants to prevent electron tunneling, a thick enough insulator has to be grown between the conducting regions, but if the insulator is too thick it increases parasitic heat conduction too much lowering significantly the device performance. Usually in com-

pound semiconductor materials with  $\varepsilon_g \cong 1 \text{ eV}$ , tunneling can occur if the barrier thickness is less than five nanometers. [7]

Interfaces may have a significant impact on thermal conduction at nanoscale. However, while in many cases interface resistance can be ignored at nanostructures this is not the case due to their high surface to volume ratio. Currently thermal resistance at interfaces is modeled with many different approaches, of which none completely describes all effects associated with heat conduction at interfaces and are also not in good agreement with current experimental data. Neither of them takes into account such important factors as inelastic scattering due to the point defects, interfacial roughness, and influence of electrical carriers. They do not also include the detailed consideration of strain at interfaces. [7, 8]

If the superlattice period is smaller than the phonon mean free path, phonons must be treated as waves, whose interactions with superlattices are governed through of a form of Bragg's law. With nanostructures, especially superlattices, it is possible to manipulate phonon dispersion and change the number of phonon modes. The goal of these operations is to reduce phonon overall group velocity. Some advantage can also be gained by increasing phonon interactions to form phononic bandgaps. One way to build them is to use alternating layers of materials with different acoustic properties analogously to constructing photonic bandgap. The ultimate goal of all modifications to phonon transport is to reduce thermal conductivity. [7]

Increased phonon confinement could also be used to increase scattering rates, which would then decrease  $\lambda_L$ . Different approaches might be necessary to block phonon transport in different parts of phonon spectrum to minimize thermal conductivity. There is much interest to thermal transport perpendicular to the superlattice plane as some experimental results show significantly lower thermal conductivity than alloy with random composition from materials used in the superlattice. As explanation superlattice has been compared with Fabry-Perot interferometer because only a few phonon frequencies can pass through. [7, 8]

Good thermoelectric material is a compromise between the high mobility and high effective mass of charge carriers. The density of states effective mass ( $m_d^*$ ) is the effective mass appearing in this context and it grows with the narrow and flat bands, which have a large density of states in Fermi-surface. This can be deduced from equations in section 2.1 as they state that effective mass is inversely proportional to the curvature of the bands. [10]

### 3. Materials

Thermoelectric phenomena were initially observed in metals, but in the mid-1900's the use of semiconductors began because of their large thermoelectric coefficients. It was quickly realized that by adding an appropriate amount of another material, which has a similar crystal structure, thermoelectric properties were improved significantly. It is known that large average atomic weight materials have lower thermal conductivity due to the decreased sound velocity in the crystal caused by the increased density. The lowest possible thermal conductivity for bulk materials is known by term 'alloy limit', because alloys usually have the lowest thermal conductivity. Atomic substitutions in alloys cause heavy phonon scattering known as alloy scattering.

Especially in power generation applications the largest possible temperature difference is required to achieve maximum performance, but the operational temperature range of thermoelectric materials is usually quite narrow indicating that the use of many different materials is in general necessary.

In thermoelectric materials, one can observe only one type of charge carriers, otherwise their movements cancel out the generated voltage [10]. Current thermoelectric materials are usually heavily doped (degenerate) compound semiconductors, because their thermal conductivity does not change much as a function of doping while electric conductivity will increase significantly and they possess a high Seebeck coefficient. In some applications, such as thermometers, metals are useful thermoelectric materials, but one of the best thermoelectric materials is bismuth telluride ( $\text{Bi}_2\text{Te}_3$ ). In Figure 8 the parameter  $zT$  as a function of temperature for some well-known thermoelectric materials is shown.

(image removed due copyright, originally figure 2 at [11])

Figure 8.  $ZT$  as function of temperature in state of the art materials. [11]

Both n- and p-type semiconductor materials are needed for a working device. Because at least two different materials have to be used, the contact resistance can cause problems, but it can be avoided by selecting materials whose electrical properties are close to each other. Good thermoelectric material parameters do not guarantee excellent device performance, because of possible losses at thermal interfaces and also at electrical connections. Usually in thermoelectric devices both p- and n-type materials are used, having different figure of merits. In such case, the material with lower  $zT$  will be the limiting factor for the device performance.

Current material development focuses mainly on different nanomaterials, since the maximum  $zT$  of traditional materials is rather low. Material groups with complex lattice structure are another trend in search for good thermoelectric materials. Some electrically conductive polymers have the potential as thermoelectric materials. Some of the materials currently in use are not able to withstand high temperatures and some others are toxic limiting their usability.

Materials used in commercial applications, such as refrigeration and waste heat recovery, must be relatively inexpensive, and suitable for manufacturing in large quantities. The ultimate goal of these investigations is to gain better understanding of transport processes and to find materials usable in commercial applications.

### 3.1 Fabrication methods

The Czochralski method is used to produce high quality single crystal material. Crystal grows on oriented seed from melt and continues as the holder of the seed is slowly pulled up. Disadvantages of this method are the slow growth rate and high equipment cost, also the quality of crystals may be a problem as the material has no structural elements that could prevent the expansion of microcracks. [1 (ch20)]

Zone melting eliminates most disadvantages of the Czochralski method by using a vertical melt zone. Material is put into a special ampoule made of quartz or refractory glass with preliminary pyrolytic graphite coating to prevent chemical reactions between the ampoule and melted material. This ampoule moves in the vertical direction through the heater on the bot-

tom. Disadvantages are quite slow growth rate and in mass production the difficulty to ensure growth conditions which would provide an acceptable yield for thermoelements. Also stresses in ingot cause microcracks during the growth stage. Whole equipment is relatively inexpensive, but the ampoule cost is a significant part of the material cost. Ingots produced with zone melting result an insufficient yield factor for the thermoelements due to the cylindrical shape and a small diameter.

Flat cavity crystallization method was developed in 1990 to achieve substantially more favorable combination of the most important material characteristics: thermoelectric efficiency, plasticity, and cost. The ingot grown by this method has the form of plate and is polycrystalline, whose crystallites are disoriented compared to larger plate surfaces and also between crystallites. Good thermoelectric efficiency and enhanced plasticity are most probably ensured by ingot structure described previously. Materials produced with this method possess several distinguishing features such as the higher thermoelectric efficiency and increased value of maximum strain before destruction (0.25 %→0.6 %). Therefore enabling material be twisted without fractures and improving usability in devices which are subjected to stresses. [1 (ch20)]

Mechanochemical synthesis (also known as mechanical alloying [MA] or high-energy mechanical milling [HEMM]) has become a popular method for the fabrication of thermoelectric materials with novel compositions and refined microstructures. In this process balls hit to the material to be milled and the impacts break the larger chunks and the particles in the mill to smaller, but these impacts also cause chemical reactions and fuse some smaller particles together. The necessary equipment are referred as ball mills and therefore the process as ball milling.

Advantages of this method are its simplicity and also solid-state nature of the process, which allows researchers to study metastable crystalline and amorphous structures. Materials produced with these methods are in powder form and then used in the manufacturing of thermoelements either by sintering or pressing methods. By selecting correct milling conditions the fabrication of powders with a specific grain size in the nanometer scale is possible. [1 (ch19)]

Chemical alloying is a bottom-up process utilizing chemical techniques to fabricate multielemental alloys. Advantages over conventional techniques are the much lower process temperature and scalability to production of bulk materials. This technique is usually divided into two major steps. At first, the required components are simultaneously precipitated from solution with required stoichiometry. Thermal processing of the precursor comes as the second step and includes calcinations in air and the reduction in hydrogen atmosphere. The final product is usually nanocrystalline powder. Currently at least nanocrystalline skutterudites are produced with this method. [1 (ch41)]

Pressing methods offer multiple advantages over both zone melting and Czochralski method, but require the source material to be in powder form. Most important advantages of pressing methods are the high output and ability to produce thermoelements in various forms with exact dimensions. Use of extrusion method, where material heated to 80 % of its melting point is forced through a draw die (hole with wanted shape) with pressure, is spreading.



Pressing and extrusion are relatively inexpensive methods and the corresponding materials have improved strength because expansion of splitting along cleavage planes is obstructed by grain boundaries. P-type thermoelectric material can have similar a figure of merit to those produced with zone melting but the same has not been achieved for n-type materials. Thermoelements that have been produced with pressing and extrusion have a better ability to withstand impact loads and thermal stresses. [1 (ch20)]

In sintering, powder is heated below its melting point usually at a high pressure to fuse particles in powder together. The sintering process has many different variations, which are optimized for different materials or end products. Pressing methods and sintering are both powder metallurgy processes.

### 3.2 Properties of thermoelectric materials

Bismuth telluride and its solid solutions are good thermoelectric materials at room temperature and therefore suitable for refrigeration applications around 300 K. The Czochralski method has been used to grow single crystalline bismuth telluride compounds. These compounds are usually obtained with directional solidification from melt or powder metallurgy processes. Materials produced with these methods have lower efficiency than single crystalline ones due to the random orientation of crystal grains, but their mechanical properties are superior and the sensitivity to structural defects and impurities is lower due to high optimal carrier concentration. [1 (ch27)]

The required carrier concentration is obtained by choosing a nonstoichiometric composition, which is achieved by introducing excess bismuth or tellurium atoms to primary melt or by dopant impurities. Some possible dopants are halogens and group IV and V atoms. Due to the small bandgap (0.16 eV)  $\text{Bi}_2\text{Te}_3$  is partially degenerate and the corresponding Fermi-level should be close to the conduction band minimum at room temperature. The size of the bandgap means that  $\text{Bi}_2\text{Te}_3$  has high intrinsic carrier concentration. Therefore, minority carrier conduction cannot be neglected for small stoichiometric deviations. Use of telluride compounds is limited by the toxicity and rarity of tellurium. [1 (ch27)]

Jeffrey Snyder and his colleagues have shown in 2008 that with thallium doped lead telluride alloy ( $\text{PbTe}$ ) it is possible to achieve  $zT$  of 1.5 at 773 K (Heremans et al., *Science*, 321(5888): 554-557). In an article published in January 2011, they showed that replacing thallium with Sodium  $zT \sim 1.4$  at 750 K is possible (Y. Pei et al., *Energy Environ. Sci.*, 2011). In May 2011 they reported in *Nature* in collaboration with Chinese research group that  $\text{PbTe}_{1-x}\text{Se}_x$  alloy doped with sodium gives  $zT \sim 1.8 \pm 0.1$  at 850 K (Y. Pei et al., *Nature*, 473 (5 May, 2011)). Snyder's group has determined that both thallium and sodium alter the electronic structure of the crystal increasing electric conductivity. The Snyder group also claims that selenium increases further electric conductivity and also reduces thermal conductivity. These works show that other bulk alloys have also potential for improvement, which could open many new applications for thermoelectrics.

$\text{Mg}_2\text{B}^{\text{IV}}$  ( $\text{B}^{\text{IV}} = \text{Si, Ge, Sn}$ ) compounds and their solid solutions are good thermoelectric materials and their figure of merit values are at the level with established materials. Due to the lack of the systematic studies about their thermoelectric properties suitability of these mate-

rials, and in particular their quasi-ternary solutions, for thermoelectric energy conversion remains in question. [1 (ch29)]

The appropriated production methods are based on direct comelting but mechanical alloying has also been used. During synthesis, magnesium losses due to evaporation and segregation of components (especially for  $\text{Mg}_2\text{Sn}$ ) need special attention. Directed crystallization methods can produce single crystalline material. Solid solutions and doped compounds have to be annealed in order to get homogeneous samples. At 800 K  $\text{Mg}_2\text{Si}_{1-x}\text{Sn}_x$  may have a figure of merit about 0.9 as can be seen from Figure 9. [1 (ch29)]

(image removed due copyright, originally figure 29.12 at [12])

Figure 9. Figure of merit for some  $\text{Mg}_2\text{Si}_{1-x}\text{Sn}_x$  solid solutions. Curves 1-3,  $\text{Mg}_2\text{Si}_{0.7}\text{Sn}_{0.3}$  (various electron concentrations); curve 4,  $\text{Mg}_2\text{Si}_{0.8}\text{Sn}_{0.2}$  and  $\text{Mg}_2\text{Si}_{0.6}\text{Sn}_{0.4}$  (curve 5). [12]

Silicon-germanium alloys are currently the best thermoelectric materials around 1000 °C and are therefore used in radioisotope thermoelectric generators (RTG) and some other high temperature applications, such as waste heat recovery. Usability of silicon-germanium alloys is limited by their high price and in addition,  $zT$  is also only in the mid-range ( $\sim 0.7$ ).

Higher silicides seem promising materials for thermoelectric energy conversion, because their figure of merit is at the level with materials currently in use and they are mechanically and chemically strong and therefore can often be used in harsh environments without any protection. More detailed studies are needed to assess their potential in thermoelectrics and possibly to find a way to increase their figure of merit. Some of possible fabrication methods are Czochralski and floating zone for single crystals and hot pressing and sintering for polycrystalline. [1 (ch31)]

Inorganic clathrates have a general formula  $\text{A}_x\text{B}_y\text{C}_{46-y}$  (type I) and  $\text{A}_x\text{B}_y\text{C}_{136-y}$  (type II), in these formulas B and C are group III and IV atoms, respectively, which form the framework where “guest” atoms A (alkali or alkaline earth metal) are encapsulated in two different polyhedra facing each other as shown in Figure 10. The differences between types I and II comes from number and size of voids present in their unit cells. Transport properties depend lot on the properties of the framework, but tuning is possible through the “guest” atoms. [1 (ch32-33), 13]



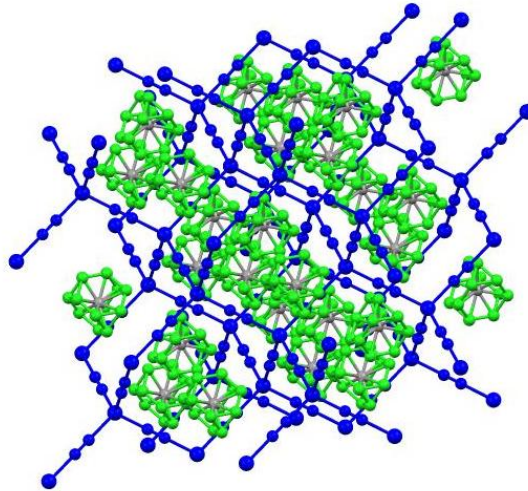


Figure 10. Crystal structure of type I clathrates. Credit: Smokefoot/[CC-BY-SA-4.0](https://creativecommons.org/licenses/by-sa/4.0/), Source: [https://commons.wikimedia.org/w/index.php?title=File:Cd\(CN\)2CCl4.jpg&oldid=238443674](https://commons.wikimedia.org/w/index.php?title=File:Cd(CN)2CCl4.jpg&oldid=238443674)

The most direct approach to the synthesis and optimization of thermoelectric properties of semiconducting type I clathrates is substitutional doping, where some framework atoms are replaced with dopant atoms. In addition, powder metallurgical and crystal growth techniques have been used in the synthesis of clathrates. The structural and chemical properties of clathrates enable the optimization of their transport properties with stoichiometry.

Type II materials should be investigated in future because their structure allows a partial filling of the polyhedron enabling a better tuning of the electrical properties and therefore a better control of the doping level. Partially filled variant can also be synthesized as semiconducting or even insulating. [1 (ch32-33)]

Blake et al have predicted  $zT \sim 0.5$  at room temperature and  $zT \sim 1.7$  at 800 K for optimized compositions. Kuznetsov et al measured electrical resistance and Seebeck coefficient for three different type I clathrates above room temperature and by estimating high temperature thermal conductivity from the published low temperature data they obtained  $zT \sim 0.7$  at 700 K for  $\text{Ba}_8\text{Ga}_{16}\text{Ge}_{30}$  and  $zT \sim 0.87$  at 870 K for  $\text{Ba}_8\text{Ga}_{16}\text{Si}_{30}$ . [1 (ch32-33)]

The composition of skutterudites corresponds to the chemical formula  $\text{ReTm}_4\text{M}_{12}$ , where Re is a rare-earth metal, Tm a transition metal and M a metalloid, which are chemical elements whose properties are between metals and nonmetals such as phosphor, antimony, or arsenic. These materials could be potential in multistage thermoelectric devices as it has been shown that they have  $zT > 1.0$ , but their properties are not well known and optimization of their structures is under way. In Figure 11 skutterudites are compared with some other TE-materials. [1 (ch34)]

(image removed due copyright, originally figure 34.9 at [1])

Figure 11.  $ZT$  as function of temperature for various TE-materials. N-type skutterudites are represented by solid squares and filled p-types with solid circles. [1 (ch34)]

Interest towards oxides as thermoelectric materials was reawakened in 1997 when  $\text{Na}_x\text{CoO}_2$  was found to be a strong candidate for thermoelectric material. Some advantages of oxides

are their thermal stability, nontoxicity and high oxidation resistance. Research on oxides as thermoelectric materials is ongoing, but it seems that in order to simultaneously control both the electric and phonon systems nanostructures have to be used. Some layered oxide materials, which are built from several layers, might have  $zT \sim 2.7$  at 900 K. If these layers have the same stoichiometry, they will be stacked so that the same atoms will not be positioned on top of each other. [1 (ch35)]

Half Heusler alloys have potential for high temperature power generation applications especially as n-type material. These alloys have three components that originate from different element groups or might even be a combination of elements in the group. Two of the groups are composed of transition metals and the third group consists of metals and metalloids. Currently only n-type material is usable in thermoelectrics but some sources claim that they have achieved  $zT \sim 1.5$  at 700 K, but according to other source only  $zT \sim 0.5$  at 700 K (Figure 12) has been achieved. They state that primary reason for this difference is the disagreement between thermal conductivities measured by different groups. These alloys are relatively cheap and also have a high power factor. [14]

(image removed due copyright, originally figure 3 at [14])

Figure 12.  $ZT$  as function temperature for following Sb doped half-Heusler alloys:  $\text{Hf}_{0.75}\text{Zr}_{0.25}\text{NiSn}_{0.975}\text{Sb}_{0.025}$ ,  $\text{Hf}_{0.60}\text{Zr}_{0.25}\text{Ti}_{0.15}\text{NiSn}_{0.975}\text{Sb}_{0.025}$ ,  $\text{Hf}_{0.75}\text{Zr}_{0.25}\text{Ni}_{0.9}\text{Pd}_{0.1}\text{Sn}_{0.975}\text{Sb}_{0.025}$ . [14]

Some electrically conducting organic materials may have a higher figure of merit than existing inorganic materials. Seebeck coefficient can be even millivolts per Kelvin but electrical conductivity is usually very low resulting small figure of merit. Quasi one-dimensional organic crystals are formed from linear chains or stacks of molecules that are packed into a 3D crystal. It has theoretically been shown that under certain conditions some Q1D organic crystals may have  $zT \sim 20$  (Figure 13) at room temperature for both p- and n-type materials. In the Thermoelectrics Handbook chapter 36.4 this has been accredited to an unspecified interference between two main electron-phonon interactions leading to the formation of narrow strip of states in the conduction band with a significantly reduced scattering rate as the mechanism compensate each other causing high  $zT$ . [1 (ch36)]

(images removed due copyright, originally figures 36.2 and 36.3 at [1])

Figure 13. Calculated  $zT$  for p-type band on the left and on the right for s-type band,  $D$  describes the carrier impurity scattering. [1 (ch36)]

With functionally graded materials, it is possible to improve the conversion efficiency of existing thermoelectric materials. These materials have a non-uniform carrier concentration distribution and in some cases also solid solution composition. In power generation applications the temperature difference can be several hundred degrees and therefore devices made from homogeneous materials have some part that operates at the temperature where  $zT$  is substantially lower than its maximum value. This problem can be solved by using materials whose transport properties vary along their length thus enabling substantial improvements to the operating efficiency over large temperature differences. This is possible with functionally graded materials as they have a variable carrier concentration along the length of the material, which is optimized for operations over specific temperature range (Figure 14). [1 (ch38)]

(image removed due copyright, originally figure 38.5 at [1])

Figure 14. Thermal conductivity and figure of merit as function temperature in low- and high temperatures for functionally graded  $(\text{Bi}_2\text{Te}_3)_{1-x-y}(\text{Sb}_2\text{Te}_3)_x(\text{Sb}_2\text{Se}_3)_y$  sample. [1 (ch38)]

Production methods for these materials can be divided into powder and crystal growth based techniques. Powder based techniques offer excellent ability to control and maintain desired carrier distribution. In crystal growth techniques dopants are often mixed with melt, but diffusion from gaseous phase can also be used. In the zone melting techniques disks of different materials are stacked on top of others and then materials are mixed with each other when a travelling heater causes melting. In powder techniques, either different powders are mixed with a varying ratio before melting or they are in different layers as a stack before pressing and melting.

## 4. Characterization

Thermoelectric materials are often characterized with a dimensionless figure of merit  $zT$ , which is determined from the product of electrical conductivity, the absolute temperature and the square of the Seebeck coefficient divided by thermal conductivity. Materials with  $zT > 1$  are considered as good thermoelectric materials, but most applications require at least  $zT > 2$  and when the goal is to replace compressor based refrigeration in domestic appliances  $zT > 3$  is required, which corresponds to approximately thirty percent of the theoretical maximum known as the Carnot efficiency (Figure 15).

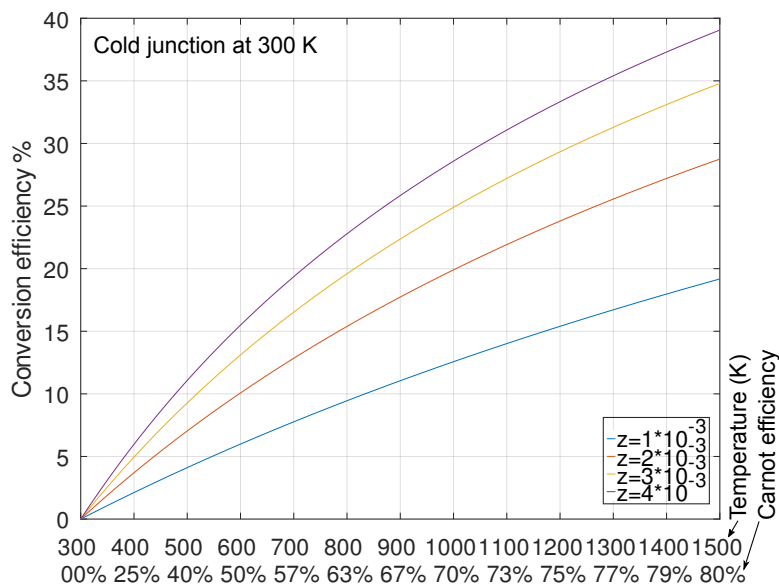


Figure 15. Conversion efficiency for thermocouple as function of temperature and figure of merit.

### 4.1 Electrical measurements

The main error sources in electrical resistivity measurements are electrical contacts to the sample and the Peltier effect by a measurement current. Because thermoelectric materials are usually semiconductors, contacts are typically metal-semiconductor interfaces. Possible oxidation of sample surfaces makes good contacts difficult to achieve. In addition, contacts often

form p-n-junctions, which can cause nonohmic voltages that lead to erroneous resistivity measurements.

Effects of Seebeck induced voltage are minimized by fast (2-3 s) measurement or/and it can be subtracted out by switching the current direction. Therefore, the electrical conductivity of thermoelectric materials should be measured by using AC or rapidly switched DC voltage. Resistivity of thin samples is usually measured with four-point techniques using collinear and evenly spaced needles as probes. Hall measurement is used determine carrier densities and mobilities. The same error sources and issues as in the measurement of bulk samples exist. [1 (ch22-24)]

## 4.2 Thermal measurements

Various methods for measuring the thermal conductivity of materials exist, but an uncertainty that is lower than 5 % is difficult to achieve due to the multiple possible error sources. One major error source is the heat transfer between the sample and surroundings. The actual method could be radiative, convection, conduction through gaseous medium and conduction through leads attached to the sample.

Heat losses by radiation are governed by Stefan-Boltzmann law, which is given by only two parameters that are the area and emissivity. It means that there is very little one can do to eliminate this effect. Heat transfer due to convection and conduction through gaseous medium can be limited by performing measurements in vacuum. Conduction through leads can be minimized by using long leads that have a small diameter with sufficient thermal anchoring. [1 (ch22-23)]

One popular technique for thermoelectric materials is a  $3\omega$ -method, in which thin metal strip evaporated on the sample acts as heat source and a thermometer. The heater is driven with AC current at frequency  $\omega$ , which causes heat source to oscillate at frequency  $2\omega$ . By monitoring AC voltage as a function of the frequency of the applied AC current thermal conductivity can be determined. The measured voltage will contain both  $\omega$  and  $3\omega$  components, because the Joule heating of the film causes small perturbation to its resistance with frequency  $2\omega$  as stated in the following equation  $V = IR = I_0 e^{i\omega t} \left( R_0 + \frac{\delta R}{\delta T} \Delta T \right) = I_0 e^{i\omega t} (R_0 + C_0 e^{i2\omega t})$ ,  $C_0$  is constant. Thermal conductivity is determined by the linear slope of  $\Delta T$  vs.  $\log(\omega)$  curve. [1 (ch23)]

The main advantages of the  $3\omega$ -method are minimization of radiation effects and easier acquisition of the temperature dependence of the thermal conductivity than in the steady-state techniques. Although some expertise in thin film patterning and microlithography is required, this technique is considered as the best pseudo-contact method available. [1 (ch23)]

Measuring thermal conductivity of thin films causes many additional difficulties compared with bulk samples. Anisotropy is common in thin films and therefore thermal conductivities in cross-plane perpendicular to the surface and in plane are not the same. These factors have to be taken into account, but with extremely thin films such methods that are even more sophisticated are needed to achieve accurate results.

Radiative heat losses are a bigger problem than in bulk samples due to the larger surface to volume ratio, but one can try to minimize these losses by radiation shielding or reflecting mirrors. Heat losses through electrical connections of temperature sensors and heaters are a major problem because they can be of the same order of magnitude than the heat flux through the films. By performing measurements at low pressure ( $<10^{-5}$  mbar) the heat losses by conduction and convection to surrounding gas can be eliminated. Schematic of the thin film thermal conductivity measurement setup is shown in Figure 16. [1 (ch24)]

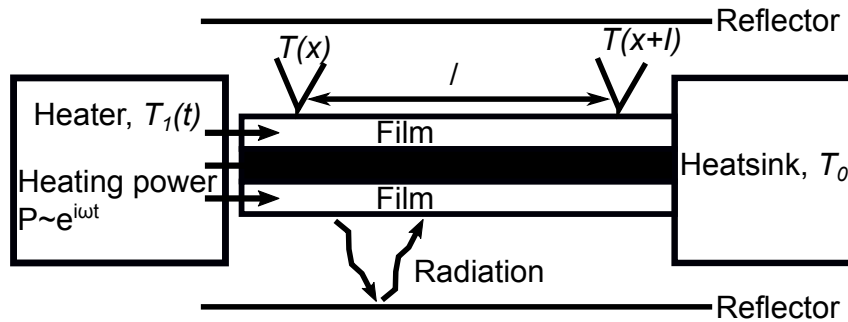


Figure 16. Setup for measuring in-plane thermal conductivity of thin films on substrate.

Great demand for methods to investigate nanoscale thermal transport exists in IC industry alone but these techniques are also needed to provide experimental data for increasing theoretical understanding of nanoscale transport mechanism. Several possible methods exist, but each of them contains several challenging practical issues. [8]

The time domain thermoreflectance method (TDTR) (schematic in Figure 17), which is also known as picosecond thermoreflectance, is a direct way to measure thermal diffusion at nanoscale. In this method the sample surface is heated using shorter than picosecond pulses from a mode locked laser, whose output is split into two beam paths, being the “pump” beam and the “probe” beam. The heating causes thermal stresses around the spot where the laser pulse hits changing the properties of the interface. The reflected energy from a series of pulses from the probe beam are used to monitor the decay of near surface temperature. Thermal conductivity and interfacial thermal resistance are then determined by comparing the experimental cooling curve with the theoretical model and optimizing the free parameters. [8]

(image removed due copyright, originally figure 16 at [8])

Figure 17. Schematic of the TDTR and picosecond acoustics apparatus. [8]

Scanning thermal microscopy (SThM) (Figure 18) can be used to probe directly local temperature and thermal transport mechanism in nanostructures. Localized heat transfer between a sharp tip and sample surface changes the tip temperature, which was usually measured with a thermocouple in the past, although some other techniques have also been developed. Nowadays the temperature sensor is most often placed on the very apex of the tip and cantilever-type probes similar to ones used in atomic force microscopes (AFMs) are used. The biggest problems with this configuration are in the fabrication of the temperature sensor to AFM tip with a method that is compatible with mass production.

A spatial map of the tip-sample heat transfer is acquired by scanning the tip across the sample surface. If the tip is at local equilibrium with the sample, spatial temperature distribution on

the sample surface is obtained. Local thermal properties can be obtained by determining temperature change for a known heat flux. Spatial resolution is currently 30-50 nm, which is also length scale where thermal transport phenomena can be studied. [8]

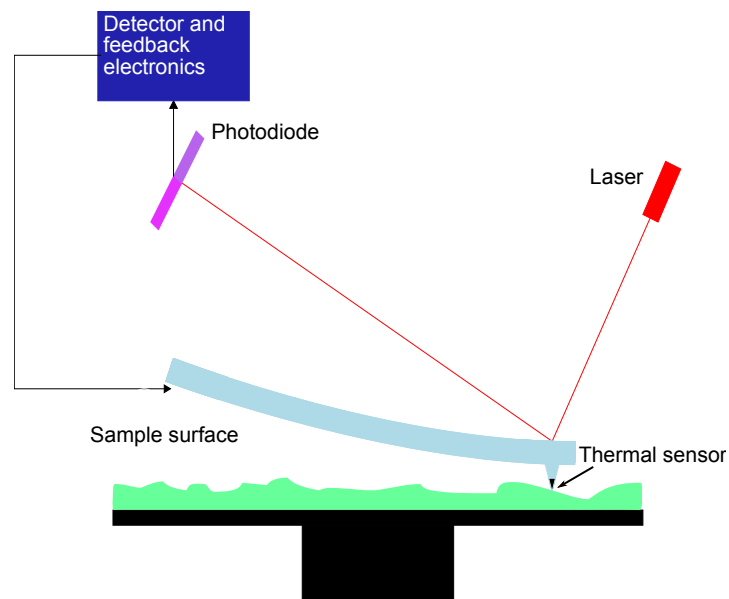


Figure 18. Schematic of cantilever-type SThM to simultaneous mapping of surface topography and temperature distribution.

### 4.3 Bands and crystal structure

Coherent optical methods have long been used in the measurements of lifetimes of optical phonons. The transport measurements with optically generated coherent phonons, particularly the acoustic modes, could be used to determine the mean free path providing an alternative to the conventional thermal methods. These coherent monochromatic phonon beams can be generated by different techniques that combine laser and suitable transducer, the laser can operate at both the continuous or pulsed mode. Longitudinally polarized phonons in 1-5 GHz range can be generated by the continuous wave laser induced thermomodulation. Excitation of layered structures with an ultrafast (subpicosecond) laser enables phonon frequencies up to  $\sim 0.5$  THz. [8]

In addition to standard material parameters, often information also about electronic band-structure, crystal structure and phonon bands are wanted. Crystal structure is usually investigated with various diffraction and interference methods from either a powder or a bulk sample. Diffraction experiments with low energy electrons and atomic beams have to be conducted in ultra high vacuum on clean surfaces. One of most important applications of neutron diffraction is the study of the order-disorder phase transitions. Transmission electron microscopy (TEM) is an appropriate method especially in structural studies of nanomaterials, but it can also be used with bulk materials. [2]

With Raman spectroscopy, properties of phonons and bonds in solids can be investigated. Photoemission spectroscopy is one of the most important methods for investigation of band structures and the density of states. The effective masses of electrons and holes in semicon-



ductors can be determined with cyclotron resonance, but measurement has to be conducted at liquid helium temperatures and crystals have to be highly perfect. [2]

#### 4.4 Thermoelectric properties

Peltier and Seebeck coefficients can experimentally be determined only for material pairs. The Seebeck coefficient ( $S$ ) is determined by measuring the voltage between the ends of the conductor, when the temperature difference between the ends is known. It is believed that the best way to measure  $S$  of bulk samples is to measure resistivity simultaneously in same measurement setup. The material parameters are temperature dependent, so in the measurements the used temperature range must be taken into account.

After material properties are known next step is to measure performance of the module, which means measuring voltage, current and conversion efficiency. The conversion efficiency of modules (power out/heat in) can be tested by sandwiching the module between the heater and the heat sink with a heat flow meter and then measuring the power output from the module. The system used usually includes also two thermocouples to measure temperatures on both sides of the module, which are integrated into ceramic plates. Losses in the heat transfer from the heater to the module are minimized by application of thermal crease and one graphite sheet.

### 5. Thermoelectric phenomenon in micro and nanoscale

It is known that with nanostructures, the thermoelectric figure of merit  $zT$  can be multiplied, and even hundred-fold increase has been reported in silicon nanowires ( $zT \sim 1$  at 200 K possible) compared with bulk silicon [15]. In nanomaterials, thermal conductivity can be reduced substantially below the ‘alloy limit’, and actually the lower limit for the thermal conductivity is still unknown. This limit will be non-zero because movement of every single phonon can not be blocked and charge carrier will also transport some heat. In nanowires, the electron density depends only on the doping level and is the same as in similarly doped bulk material.

The effects of confinement on scattering and thermoelectric coefficients have been discussed in section 2.4 and it was noticed that it is possible to increase the value of the Seebeck coefficient and modify scattering compared with bulk materials. Increased scattering and reduced mean free path are responsible for the significantly lower lattice thermal conductivity in nanoscale. However, when modifying one transport parameter there is always risk affecting others thus reducing the performance improvement.

The power factor can be maximized by adjusting the Fermi-level and increasing temperature, but to achieve bigger increase these methods are not enough. There are a few strategies to increase the power factor beyond the bulk value: the use of quantum confinement to increase the magnitude of density of states (DOS), which may result in the increase of the Seebeck coefficient or increasing the number of active conduction valleys (carrier pockets) contributing to transport. [5, 7]

Confinement effects shift the energy levels of the carrier pockets and different pockets experience these effects a bit differently thus allowing the shifting of the pocket energies to similar levels. This means that the ground state energy levels of the pockets shift close to each

other so pockets whose energy levels would normally be too high for them to be populated with electrons become active. If the energy levels of the impurity are in the conduction or valence bands, they create a resonant level and a local maximum in the electronic DOS. If the Fermi level is close to this maximum, the Seebeck coefficient is expected to increase, which has been verified experimentally by Heremans and coworkers in bulk Tl doped PbTe [5].

As shown in section 2.1 the dependence between the DOS and electric conductivity originates from effective mass trough mobility and from intrinsic carrier density, which can be ignored in doped materials. Changing temperature changes the Fermi-level, but often one wants to optimize the material for specific temperature range. This means that other means are necessary. One possibility is to change the doping level, which is one of the easiest practical ways to change the Fermi-level. Second way is to use quantum confinement to modify the DOS. [5, 7]

Nanostructures are not in the equilibrium state, thus creating thermodynamically stable material needed for practical devices is difficult. If nanostructured material is not thermodynamically stable, it can revert back to its bulk state during device operation losing its enhanced thermoelectric properties. [5]

Search for good thermoelectric nanomaterials is complicated because the transport properties of nanomaterials are not well understood as discussed in section 2.4. Some nanostructures enable individual tuning of transport parameters by adjusting structural parameters. Because no proper model about nanoscale transport exists, necessary adjustments for the optimal parameters cannot be predicted. These factors make the development of thermoelectric nanomaterials difficult. For commercial applications, the most potential is in nanowires, embedded nanoparticles, nanocrystalline and nanoporous materials, because they can be manufactured on a large scale at reasonable cost.

## 5.1 Fabrication of thermoelectric nanomaterials

Thermoelectric devices from nanocrystalline materials can be fabricated with same processes as devices from bulk materials. Powder based methods, especially mechanical alloying (MA) and subsequent sintering are promising methods for the production of bulk nanostructured materials. Ball milling is a widely spread method for fabricating nanocrystalline materials in powder form. These methods were discussed in chapter 3.1.

Probably most practical way to fabricate nanowire arrays is to use a template, which has parallel holes side by side. Top-down methods are impractical for nanowires that are even over 100 nm in size and practically impossible for structures that are smaller than a few tens of nanometers. Nanoporous channels as template are an interesting idea but whether or not they are suitable for mass production depends on how channels are fabricated. After the nanowires are grown, the template will be usually destroyed or in some cases wires are just released.

Nanoporous channels are often fabricated by modifying a structure of the template material with swift heavy ion bombardment so that the exposed area can be etched away. If the bombardment lasts too long, areas designated not to be etched might also get etched so it is done with a high ion flux using short irradiation time. Another possibility is the anodic etching of alumina.



Second approach to make nanowire arrays is to use self-assembled block co-polymer templates, which would then be filled with thermoelectric material. This approach allows wide selection of material and filling method options. With a simple template fabrication and by choosing the nanowire fabrication method correctly, this is probably the best fabrication method for nanowire arrays for commercial applications.

Templates can also be fabricated with top-down methods but they must contain features at the nanometer scale such as narrow ridges or grooves, where nanowires could be grown. However, these kinds of templates are most likely incompatible for fabrication nanowire arrays.

Bismuth nanowires are usually fabricated by introducing it to alumina ( $\text{Al}_2\text{O}_3$ ) templates with either by pressure injection method, vapor phase method or electrochemically. Two previous methods produce single crystal material, but with electrochemical methods only polycrystalline material can be fabricated. From these an electrochemical method is the most suitable for production due to its versatility to use it for many species. Further advantages are the means to attach good ohmic contacts with nanowire arrays and possible integration with silicon technology so that silicon wafers would act as substrates to alumina templates. Process flow for nanowire fabrication with template and a SEM picture of a filled template are shown in Figure 19. Electrodeposition can also be used at least for  $\text{CoSb}_3$  and  $\text{Bi}_2\text{Te}_3$ . [11, 1 (ch39)]

(image removed due copyright, originally figure 39.4 at [1])

Figure 19. On the left a schematic of nanowire fabrication using alumina template and on the right is a SEM picture of the template after depositing TE-material. [1 (ch39)]

Vapor liquid solid method is one widely used technique to grow one-dimensional structures from vapor phase precursors of material A, which are dissolved into liquid droplets of material B on substrate surface forming an alloy AB. After certain time A supersaturates B and if melting temperature of A is lower than that of B, nanowire from A will form as A starts to precipitate from a droplet. It allows controlling the nanowire size by controlling the size of the droplets. Growth of nanowire arrays is possible but still this method does not seem to be usable for mass production. It is however usable for producing nanowires for research purposes.

## 5.2 Material classes currently under investigation

Not all nanocrystalline materials are stable, because the crystal size can grow at high temperatures ruining materials desired characteristics. In nanocrystalline material, there are many interfaces between crystals, which scatter phonons so the thermal conductivity is reduced. Phonons are confined to the grain, if their mean free path is larger than the material grain size. Measured lattice thermal conductivity in nanowires is known to depend on roughness, the method of synthesis and properties of the source material. [7]

Nanocrystalline transition metal silicides are a promising material group for thermoelectric applications, because they fulfill several criteria that are demanded from the commercial applications point of view. In some nanocrystalline transition metal silicides the power factor is higher than in the corresponding polycrystalline material but the lack of reliable data on thermal conductivity prevents the evaluation of their thermoelectric efficiency. [1 (ch40)]

One advantage of nanostructured skutterudites over normal skutterudites is their reduced thermal conductivity but further performance improvements can be achieved by using composites and by controlling the grain size, the compaction conditions of polycrystalline samples and the carrier concentration. Thermal conductivity reduction is caused by grain boundary scattering.  $ZT$  values of  $\sim 0.65$  and  $>0.4$  have been achieved with  $\text{CoSb}_3$  based samples, the former value is for 2.0 at.% Ni and 0.75 at.% Te doped material at 680 K (Figure 20) and latter for Au-composite at  $T > 700$  K. [1 (ch41)]

(image removed due copyright, originally figure 41.4d at [1])

Figure 20. Measured  $zT$  as a function of temperature for Ni, Te doped  $\text{CoSb}_3$  skutterudites. [1 (ch41)]

Due to the unique nature of graphene, engineering of thermoelectric device with extremely high Seebeck coefficient based on this material is possible. One theoretical study suggests that the Seebeck coefficient might achieve a value of 30 mV/K at room temperature and  $zT$  for their proposed device would be approximately 20. [16]

Superlattices and quantum wells can be good thermoelectric materials, but their production is too difficult and expensive for general use because of their fabrication is based on various thin film growth methods. Superlattice structures allow the independent manipulation of transport parameters by adjusting the structural parameters enabling the search for better understanding of thermoelectric phenomena in nanoscale.

Many strategies exist to decrease the superlattice thermal conductivity that are based on engineering of phonon transport. The thermal conductivity along the film plane and wire axis can be reduced by creating diffuse interface scattering and by reducing the interface separation distance, both which are caused by interface roughness. The interface roughness can be natural due to the mixing of atoms at the interfaces or artificial. Many different structure types, such as quantum dot interfaces and thin films on step-covered substrates, can act as source for artificial roughness. [11]

However while engineering interface structures for reduced phonon thermal conductivity effects to electron transport has to be taken into account because the reduced electrical conductivity could negate the advantage received from phonon transport engineering. Because electrons and phonons have different wavelengths, it may be possible to engineer the structure in such a way that phonons are scattered more diffusely at the interface than electrons. This would reduce the decrease of the electrical conductivity.

Second approach is to increase phonon reflectivity and therefore decrease the thermal conductivity perpendicular to interfaces. This can be achieved by increasing the mismatch between the materials. Some of these properties are density, group velocity, specific heat, and the phonon spectrum between adjacent layers. Interface roughness causes diffuse phonon scattering, which either increases or decreases the phonon reflectivity at the interfaces. Mismatch between bulk dispersion relations confines phonons and the confinement becomes more favorable as the difference in dispersion increases. The amount of confinement is currently unknown as only some models and experimental data exist. As with a previous method, the effects on the electrical conductivity have to be considered. [11]

In order to further reduce the thermal conductivity, the localization of long wavelength phonons can be attempted with aperiodic superlattices or composite superlattices with different periodicities. In addition, defects, especially dislocations, can be used to reduce thermal conductivity in low dimensional systems. [11]

Thermoelectric performance improvements in superlattices originate from various sources, usually at least the lattice thermal conductivity in the cross plane direction is very low but depending on the type of superlattice, the thermoelectric coefficient may also increase because the bandstructure changes. Low lattice thermal conductivity in superlattices is usually due to strong interface scattering of phonons. Electronic bandstructure in superlattices comprises the so called minibands, which appear due to quantum confinement effects. In superlattices, electronic bandstructure depends on the superlattice period so that with very short period ( $\sim 1$  nm) the bandstructure approaches the alloy limit and with long period ( $\geq \sim 60$  nm) minibands become so close to each other that they can be approximated with a continuum. [1 (ch16, 39)]

Especially in multi quantum well structures the parasitic heat conduction could cause significant performance reduction. Fortunately, the impact of this phenomenon can be reduced by choosing the distance between the quantum wells correctly.

The Seebeck coefficient can change its sign in superlattice nanowires due to the existence of minigaps as Fermi energy varies. This indicates that superlattices can be tailored to exhibit n or p-type behavior by using the same dopants as those that are used for corresponding bulk materials by carefully controlling Fermi energy or the dopant concentration. [1 (ch39)]

With nanowire arrays, it is possible to exploit semimetal-semiconductor transition due to the quantum confinement and use materials that normally would not be good thermoelectric materials in bulk form. Such elements are for example bismuth. The Seebeck effect could also be used to determine the carrier concentration and Fermi energy in nanowires. [1 (ch39)]

In quantum dot thermoelectrics, unconventional or nonband transport behavior (e.g. tunneling or hopping) is necessary to utilize their special electronic bandstructure in the transport direction. It is possible to achieve  $zT \sim 3$  at elevated temperatures with quantum dot superlattices, but they are almost always unsuitable for mass production.  $\text{Bi}_2\text{Te}_3/\text{Sb}_2\text{Te}_3$  superlattice as a microcooler has been reported to have  $zT \sim 2.4$  at 300 K. [1 (ch49)]

Nanocomposites are promising material class for bulk thermoelectric devices, but several challenges have to be overcome to make them suitable for practical applications. It is not well understood why the improved thermoelectric properties appear only in certain materials with specific fabrication processes. [5]

K. Biswas et al. report in Nature Chemistry 3, 160–166 (2011) that SrTe nanocrystals embedded in a bulk PbTe matrix so that rocksalt lattices of both materials are completely aligned (endotaxy) with optimal molar concentration for SrTe only 2 % can cause strong phonon scattering but would not affect charge transport. They report maximum  $zT \sim 1.7$  at 815 K for p-type material.

### 5.3 Use of nanoscale thermoelectrics

Current low dimensional thermoelectrics are mainly model systems for understanding the underlying concepts, which would then be applied to the production of practical systems. Nanocomposites where nanowires or nanodots would be added to host material for enhanced thermoelectric performance are considered as possible materials for commercial applications. These nanocomposites can be produced by adding nanostructured building blocks to host powder material and then using hot or cold pressing techniques or induction heating to form the composite. A direct chemical embedding of quantum dot structures to host material with good thermoelectric properties is another approach to the fabrication of practical thermoelectric material. Role of these nano-inclusions is believed to be significant but their exact role is still under investigation. [1]

Thin films can only be used with small temperature differences, which prevent their use in many applications such as turning the waste heat into electricity. Thermoelectric materials based on thin films are only suitable for cooling or as power sources of small objects. Today applications can be found mainly in optoelectronics, but in the future for example different laboratory chips require accurate temperature control, which can be realized only with integrated thermoelectric cooling. Thermoelectric cooling elements can be included in integrated circuits to cool either the entire chip or just the hottest points. One major problem is transforming the high figure of merit of material to high device ZT.

### References

- 1 Rowe, David Michael. Thermoelectrics handbook : macro to nano / edited by D.M. Rowe. Boca Raton: CRC/Taylor & Francis, 2006. ISBN 0-8493-2264-2
- 2 Ibach, Harald. ; Lüth, Hans. Solid-state physics : an introduction to principles of materials science / Harald Ibach, Hans Lüth. New York: Springer, 2009. - (Advanced texts in physics) ISBN 978-3-540-93803-3
- 3 Ferry, David K. Semiconductor transport. London: Taylor & Francis, 2000. ISBN 0-7484-0865-7 (hbk.), ISBN 0-7484-0866-5 (pbk.)
- 4 A. Bulusu, D.G. Walker. Review of electronic transport models for thermoelectric materials, Superlattices and Microstructures, Volume 44, Issue 1, July 2008, Pages 1-36, ISSN 0749-6036, DOI: 10.1016/j.spmi.2008.02.008.
- 5 A. J. Minnich, M. S. Dresselhaus, Z. F. Ren and G. Chen. Bulk nanostructured thermoelectric materials: current research and future prospects, Energy & Environmental Science, 2009, 2, 466-479, DOI: 10.1039/b822664b
- 6 Bhattacharya, Pallab. Semiconductor optoelectronic devices / Pallab Bhattacharya. Upper Saddle River (NJ): Prentice-Hall, 1997. ISBN 0-13-495656-7 (nid.)

7 Paothep Pichanusakorn, Prabhakar Bandaru. Nanostructured thermoelectrics, *Materials Science and Engineering: R: Reports*, Volume 67, Issues 2-4, 29 January 2010, Pages 19-63, ISSN 0927-796X, DOI: 10.1016/j.mser.2009.10.001.

8 David G. Cahill, Wayne K. Ford, Kenneth E. Goodson, Gerald D. Mahan, Arun Majudar, Humphrey J. Maris, Roberto Merlin, and Simon R. Phillpot. Nanoscale thermal transport, *J. Appl. Phys.* 93, 793 (2003), DOI:10.1063/1.1524305

9 Datta, Supriyo. *Electronic transport in mesoscopic systems*. New York : Cambridge UP, 1995. ISBN 0-521-41604-3, ISBN 0-521-59943-1

10 G. Jeffrey Snyder & Eric S. Toberer. Complex thermoelectric materials, *Nature Materials* 7, 105-114 (2008), doi:10.1038/nmat2090

11 Chen, G.; Dresselhaus, M. S.; Dresselhaus, G.; Fleurial, J.-P.; Caillat, T. Recent developments in thermoelectric materials, *International Materials Reviews*, Volume 48, Number 1, February 2003, pp. 45-66(22)

12 Gerald Mahan, Brian Sales, and Jeff Sharp, *Thermoelectric Materials: New Approaches to an Old Problem*, *Phys. Today* 50, 42 (1997), DOI:10.1063/1.881752

13 Gatti, C., Bertini, L., Blake, N. P. and Iversen, B. B. (2003), Guest–Framework Interaction in Type I Inorganic Clathrates with Promising Thermoelectric Properties: On the Ionic versus Neutral Nature of the Alkaline-Earth Metal Guest A in  $A_8Ga_{16}Ge_{30}$  (A=Sr, Ba). *Chemistry - A European Journal*, 9: 4556–4568. doi: 10.1002/chem.200304837

14 Slade R. Culp, S. Joseph Poon, Nicoleta Hickman, Terry M. Tritt, and J. Blumm, Effect of substitutions on the thermoelectric figure of merit of half-Heusler phases at 800 °C, *Appl. Phys. Lett.* 88, 042106 (2006), DOI:10.1063/1.2168019

15 Akram I. Boukai, Yuri Bunimovich, Jamil Tahir-Kheli, Jen-Kan Yu, William A. Goddard III & James R. Heath. Silicon nanowires as efficient thermoelectric materials, *Nature* 451, 168-171 (10 January 2008), doi:10.1038/nature06458

16 D. Dragoman and M. Dragoman, Giant thermoelectric effect in graphene, *Appl. Phys. Lett.* 91, 203116 (2007), DOI:10.1063/1.2814080